analytical chemistry

Article

pubs.acs.org/ac

Inhibitory Impact of 3′-Terminal 2′-O-Methylated Small Silencing RNA on Target-Primed Polymerization and Unbiased Amplified Quantification of the RNA in *Arabidopsis thaliana*

Feng Chen,[†] Chunhai Fan,[‡] and Yongxi Zhao*[,†]

[†]Key Laboratory of Biomedical Information Engineering of Education Ministry, School of Life Science and Technology, Xi'an Jiaotong University, Xianning West Road, Xi'an, Shaanxi 710049, P. R. China

[‡]Division of Physical Biology, and Bioimaging Center, Shanghai Synchrotron Radiation Facility, CAS Key Laboraotory of Interfacial Physics and Technology, Shanghai Institute of Applied Physics, Chinese Academy of Sciences, Yuquan Road, Shanghai 201800, P. R. China

Supporting Information

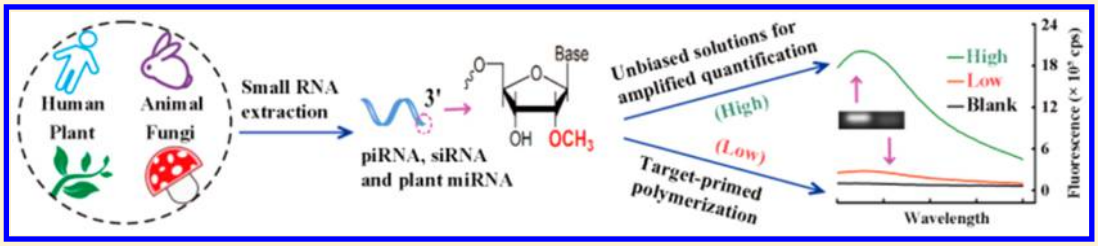

ABSTRACT: 3′-terminal 2′-O-methylation has been found in several kinds of small silencing RNA, regarded as a protective mechanism against enzymatic 3′ → 5′ degradation and 3′-end uridylation. The influence of this modification on enzymatic polymerization, however, remains unknown. Herein, a systematic investigation is performed to explore this issue. We found these methylated small RNAs exhibited a suppression behavior in target-primed polymerization, revealing biased result for the manipulation of these small RNAs by conventional polymerization-based methodology. The related potential mechanism is investigated and discussed, which is probably ascribed to the big size of modified group and its close location to 3′-OH. Furthermore, two novel solutions each utilizing base-stacking hybridization and three-way junction structure have been proposed to realize unbiased recognition of small RNAs. On the basis of phosphorothioate against nicking, a creative amplified strategy, phosphorothioate-protected polymerization/binicking amplification, has also been developed for the unbiased quantification of methylated small RNA in *Arabidopsis thaliana*, demonstrating its promising potential for real sample analysis. Collectively, our studies uncover the polymerization inhibition by 3′-terminal 2′-O-methylated small RNAs with mechanistic discussion, and propose novel unbiased solutions for amplified quantification of small RNAs in real sample.

Small silencing RNAs are short (~20−30 nucleotides) noncoding RNAs, mainly including small interfering RNAs (siRNAs), Piwi-interacting RNAs (piRNAs) and microRNAs (miRNAs).[1,2] Despite different biogenesis mechanisms, they all can specifically reduce the expression of target genes by forming RNA-induced silencing complex associated with Argonaute family proteins.[1,3] These small RNAs play diverse and significant roles in biological functions, disease states and therapeutic application of RNA interference.[4−8] Aberrant expression level of small RNAs is closely related with many physiological defects and even diseases.[1,9]

Since the first discovery in plant miRNAs in 2005,[10] 2′-O-methylation at 3′-terminal ribose has been found in siRNA,[3,11] and in piRNA of human and animals.[12] This molecular modification is thought to facilitate the recognition of small RNAs by associated proteins, and enhance stability to prevent 3′ → 5′ exoribonuclease degradation and 3′-end uridylation.[10,13] It seems that this modification does not affect the discovery and manipulation of small RNAs due to the unaltered base sequence. Nevertheless, no evidence has emerged. Oppositely, in view of its protection against enzymatic degradation and uridylation, we conjecture this structure with 3′-terminal 2′-O-methyl group may also hinder other enzymatic reaction such as polymerization. It is well-known that target-primed polymerization methods[14−17] have been widely applied for small RNAs analysis[18−25] as alternative to traditional methods.[26] The inhibition on polymerization may cause serious biased result for the detection and quantification assay of these modified small RNAs. It is an urgent need to explore this issue.

In this work, we study the impact of these modified small RNAs on enzymatic polymerization, and seek to offer novel designs for the unbiased and sensitive quantification of these modified small RNAs. Using three representative DNA polymerases (Bst 2.0 DNA polymerase, Klenow Fragment

Received: May 4, 2015
Accepted: August 5, 2015
Published: August 5, 2015

DOI: 10.1021/acs.analchem.5b01683
Anal. Chem. 2015, 87, 8758−8764

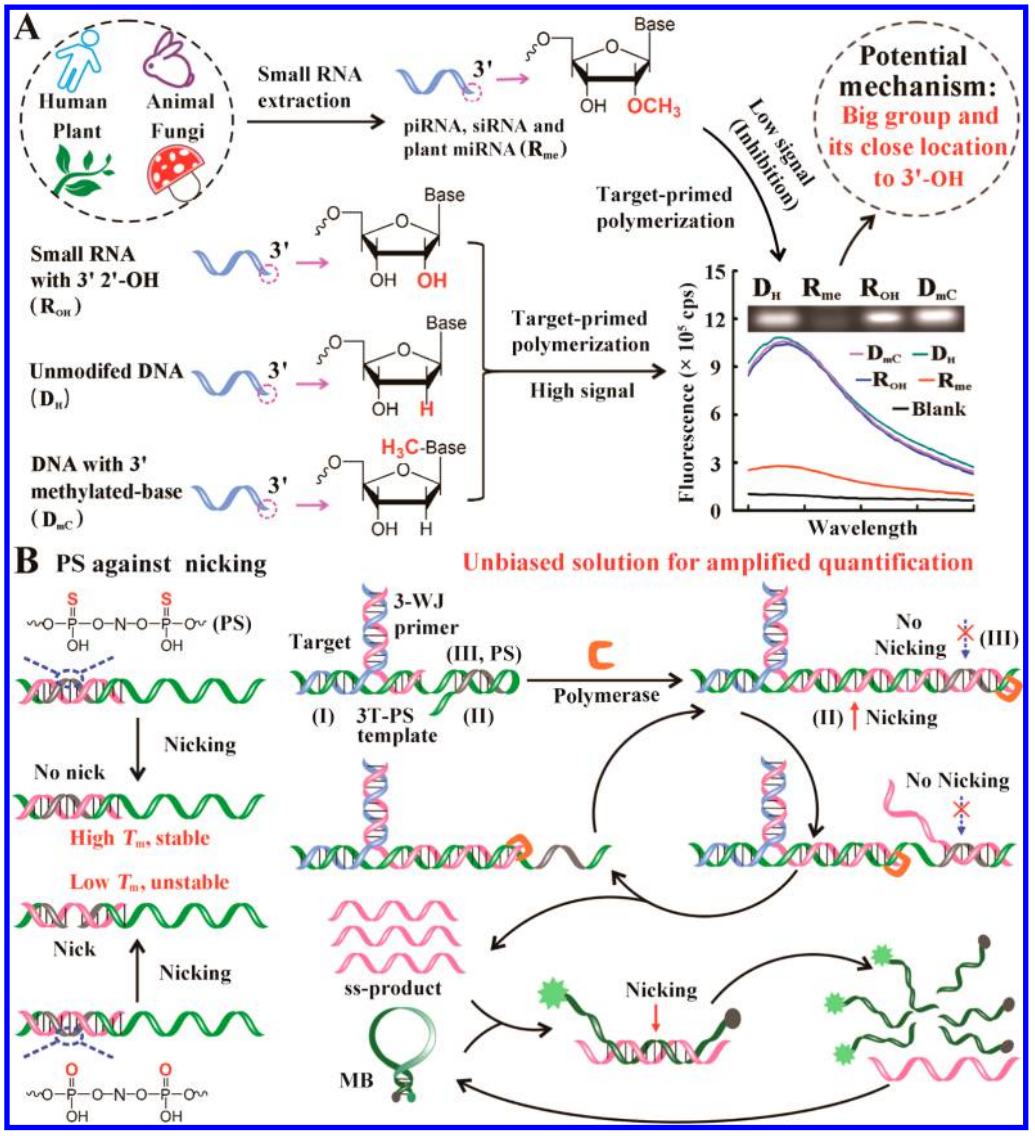

Figure 1. Illustration of the biased analysis result of 3′-terminal 2′-O-methylated small RNAs by conventional target-primed polymerization methodology. (A) Inhibition of 3′-terminal 2′-O-methylated small RNA on target-primed polymerization and amplificaiton. The base in this work is cytosine (C), and mC means C is methylated at the 5 position. R_{OH}, D_H, and D_{mC} indicate small RNA with 3′ 2′-OH, unmodified DNA and DNA with 3′ methylated base, respectively. Target-primed polymerization means the polymerization process using target (small RNA) as primer, result of which is shown in gel electrophoresis image. And the result of subsequent SDA is depicted as the fluorescence spectra. The inhibitory impact on target-primed polymerization by 3′-terminal 2′-O-methylated small silencing RNA is presented and the potential mechanism is explored. (B) Scheme of phosphorothioate (PS) against nicking (left) and PS−PBN combined with 3-WJ structure (right) for the unbiased recognition and sensitive detection of small RNAs. The 3T-PS template contains three important domains (I is for the recognition of target; II and III are the complementary recognition sequences for nicking enzyme). The blue dashed arrow represent the failing nicking of phosphorothioate site, whereas the two red arrows show the successful nicking. MB is the abbreviation of molecular beacon.

exo⁻, and Vent exo⁻ DNA polymerase), systematic experiments have been carried out. Despite diverse inhibition level, remarkable suppression behavior was observed in target-primed polymerization catalyzed by all DNA polymerases, raising biased analysis results. Significant effort was made for understanding the potential mechanisms of above polymerization suppression. Furthermore, using base-stacking hybridization and three-way junction (3-WJ) structure, we proposed two solutions to circumvent this suppression impact and realize unbiased recognition of the modified small RNA. To improve the sensing performance, a creative amplified strategy, phosphorothioate-protected polymerization/binicking amplification (PS−PBN), has been proposed by utilizing an artificially designed trifunctional stem-loop template which contains a hemiphosphorothioate nicking site. This method has been applied for the available detection of small RNA samples extracted from *Arabidopsis thaliana*, demonstrating its promising potential for real sample analysis.

EXPERIMENTAL SECTION

Materials and Reagents. Bst 2.0 DNA polymerase, Klenow Fragment exo⁻(KF⁻), Vent exo⁻DNA polymerase and nicking enzyme Nt.BbvC I were purchased from New England Biolabs Ltd. RNase inhibitor, DNA ladder, and commercial RNA extraction kits (RNAiso for small RNA) were purchased from Takara Biotechnology Co., Ltd. (Dalian, China). HPLC-purified miRNAs were synthesized by Invitrogen (Shanghai, China), and the other oligonucleotides and

DOI: 10.1021/acs.analchem.5b01683
Anal. Chem. 2015, 87, 8758−8764

deoxynucleotide triphosphates (dNTPs) mix were obtained from Sangon Biotechnology Co., Ltd. (Shanghai, China). The nucleic acid sequences are shown in Table S1. All solutions were prepared and diluted by RNase-free sterilized water.

Instruments. LightCycler 96 (Roche Applied Science, Mannheim, Germany) was used to record real-time fluorescence signal and melting curves. The gel was imaged by Syngene G:BOX Imaging System (Syngene System, Cambridge, UK). Fluorescence measurements were carried out by using a FluoroMax-4 fluorescence spectrometer (Horiba Jobin Yvon, Edison, NJ). The emission spectra were obtained from 510 to 570 nm with an excitation wavelength of 495 nm at room temperature in steps of 1 nm. The fluorescence intensity at 518 nm was chosen as the optimal experimental conditions. The slit widths of both excitation and emission were set at 5 nm.

PS−PBN Assay. 3T-PS template with three functional domains was used in PS−PBN instead of 3-WJ template. To form the heteroduplex of 3T-PS template and 3T product, a mixture containing 100 nM 3T-PS template and 25 nM 3T product in the annealing buffer (10 mM Tris-HCl, 50 mM NaCl, 1 mM EDTA, pH = 7.8) was heated to 95 °C for 5 min and then 45 °C for another 20 min. It was stored at 4 °C for further use. A standard PS−PBN reaction (20 μL, 1 × NEBuffer 4) contains variable amounts of miR156a, 10 nM 3-WJ primer, 10 nM above heteroduplex, 250 nM MB, 0.5 units of KF-, 2.5 units of Nt.BbvCI, 16 units of RNase inhibitor and 0.2 mM dNTPs. The mixture was performed with incubation for 30 min at 37 °C.

RESULTS AND DISCUSSION

As shown in Figure 1A, small RNAs samples from varied species contain 3′-terminal 2′-O-methylated one (piRNA, siRNA, or plant miRNA). These modified small RNAs induces observably low signal response in target-primed polymerization reaction by Bst 2.0 DNA polymerase, whereas other three control samples (R_{OH}, D_H, and D_{mC}) prime high polymerization signal (gel electrophoresis image, Figure 1A). Using SYBR Green I as fluorescent reporter, we real-time examined the impact of 3′-terminal 2′-O-methylated small RNA on polymerization reaction. It can be seen in Figure 2A, fluorescence signal by methylated sample increases slowly, whereas unmethylated one resulted in saturated signal value very fast. Corresponding melting curves are recorded to verify the generation of polymerization product (Figure 2B). After that, strand displacement amplification (SDA), a representative target-primed polymerization method for small RNA analysis, was employed to monitor the suppression impact (Figure 2C and 2D). The fluorescence enhancement of methylated sample is slower than that of unmethylated one. All of above results confirmed the suppression behavior in polymerization reaction as well as subsequent amplified process by 3′-terminal 2′-O-methylated small RNA.

A quantitative and comprehensive analysis of above inhibition on SDA was carried out using molecular beacon (MB) owing to its high signal-to-noise ratio. The signal value of methylated sample is only about 3 folds of the background, which is far below that by unmethylated one (Figure 3A and 3D). Since Klenow Fragment exo$^-$ and Vent exo$^-$ DNA polymerase are also involved in polymerization-based methods for small RNAs analysis, the impact on their polymerization reaction were successively investigated. Similar results as that of Bst 2.0 DNA polymerase were obtained (Figure 3B, 3C and

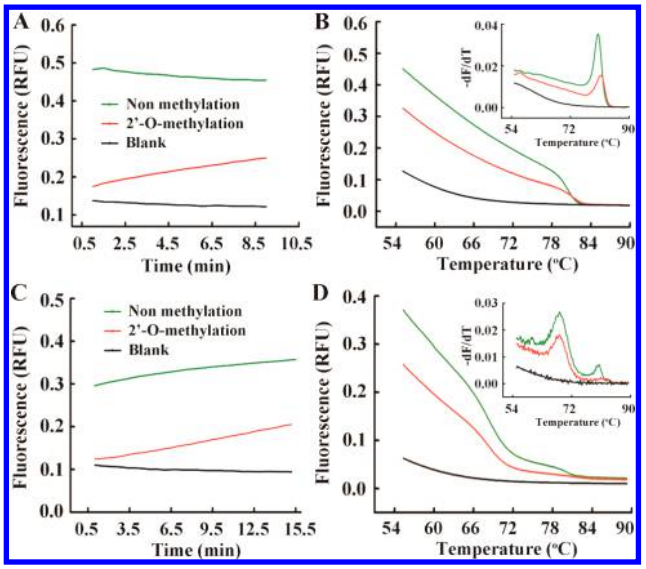

Figure 2. Real-time fluorescence analysis of the inhibition by 3′-terminal 2′-O-methylated small RNA on target-primed polymerization (A) and SDA (C). B and D are the melting curve of A and C, respectively. Two peaks are observed in (D). The one of about 80 °C presents the full duplex template as that in (B), whereas the other one indicates the duplex formed by the hybridization of SDA product and template.

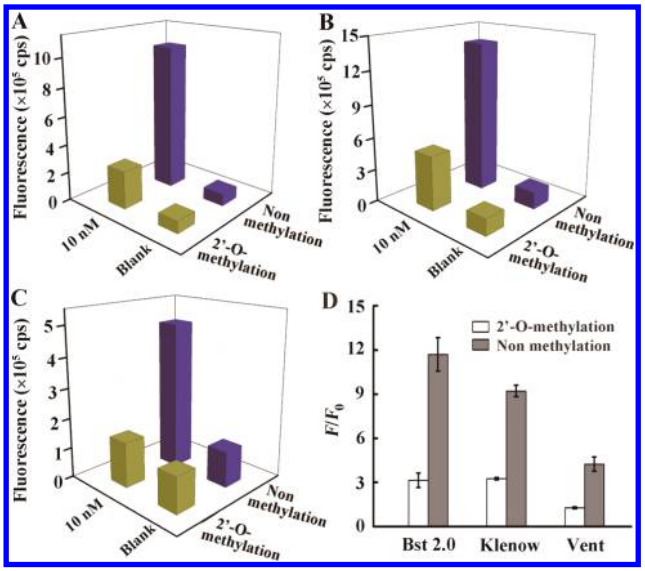

Figure 3. Inhibition of 3′-terminal 2′-O-methylated small RNA on SDA catalyzed by three representative DNA polymerase (A, Bst 2.0 DNA polymerase; B, Klenow Fragment exo$^-$; C, Vent exo$^-$ DNA polymerase) using MB as reporter. (D) The corresponding fluorescence enhancement. F and F_0 represent the fluorescence intensity of signal and blank, respectively.

3D). Furthermore, the concentration-dependent effect on such suppression reaction was investigated. We expect that increasing the small RNA concentration may improve the polymerization efficiency. However, marked decrease of fluorescence intensity by 2′-O-methylated small RNA is still observed as compared to unmodified sample (Figure S1). Different buffer conditions for SDA were also employed to evaluate the inhibition by this modified small RNA. Similar conclusion is obtained despite the various fluorescence intensity (Figure S2). Evidently, all these results indicate the universality

DOI: 10.1021/acs.analchem.5b01683
Anal. Chem. 2015, 87, 8758−8764

of such suppression behavior, and imply the shortcoming of conventional target-primed polymerization methodology when applied to modified small RNAs anaysis.

To fully explore the mechanism of aforementioned inhibition, other three kinds of nucleic acids (R_{OH}, D_H, and D_{mC}) are employed as comparison. Though they share the same sequence, their structure of 3′-terminal nucleotide are different (Figure 1A). Besides the gel electrophoresis analysis result of target-primed polymerization reaction (Figure 1A), fluorescence response of SDA triggered by these four targets are also compared (Figure 1A and Figure S3). Only the 2′-O-methylated small RNA leads to low fluorescence signal, whereas the unmodified ones (R_{OH} and D_H) and even methylated D_{mC} can induce high signal. The main structure difference between these nucleic acids is the modified group size and spatial location. Methyl group (in R_{me} and D_{mC}) is bigger than hydroxyl (in R_{OH}) and hydrogen (in D_H). And the 2′-O-methyl group (R_{me}) is directly adjacent to 3′−OH on the ribose, whereas the methyl group of D_{mC} is located on the base (far away from 3′-OH). It is well-known that DNA polymerases recognize 3′−OH to start polymerization reaction. Therefore, we speculate that the steric hindrance (including big group size and close location) of 2′-O-methy group may cause the failing of polymerization reaction. This mechanism might be also appropriate to explain the resistance of nuclease-mediated degradation and uridylation by 3′-terminal 2′-O-methylation in vivo. It is worthy to point out that the varied inhibition in three DNA polymerases may be owing to the difference of enzymatic structures and their interaction with primer-template duplex.[27,28] As we known, it is the first time to study such suppression behavior and reveal its potential mechanism.

Since target-primed polymerization methods have been widely applied for small RNAs analysis and detection, above-mentioned inhibition will lead to biased results. Herein, we proposed two novel designs to avoid such inhibition impact and achieve unbiased analysis of small RNA. One of them is based on base-stacking hybridization (left of Figure 4A). It is well-known that the base-stacking interaction significantly enhance the stability of duplex via adjacent base pairs.[29−33] In this solution, an unmodified primer with 5-bp complementary to template is employed for polymerization reaction. In the absence of target small RNA, the primer cannot form stable duplex with template to start polymerization reaction. However, when target small RNA hybridizes with template adjacently to primer, stability of such duplex is strongly increased, resulting in polymerase-catalyzed reaction. As shown in Figure 4A, methylated target induces signal value as high as that of unmethylated one. Another solution achieves the unbiased output on the basis of 3-WJ structure (left of Figure 4B).[34,35] The 3-WJ primer used here is able to form stable structure with template in the presence of target small RNA to prime polymerization reaction, whereas polymerization reaction fails to happen without target. High signal by methylated target is also observed in Figure 4B. Obviously, the key point of these two solutions is that to introduce assistant primers instead of using 3′-terminal 2′-O-methylated RNA as primer for polymerization reaction.

To further improve the assay performance, a creative amplified strategy, PS−PBN, has been developed for the first time (right of Figure 1B). It is mainly based on the hypothesis that nicking enzyme cannot cut the phosphorothioate sequence in recognition site (left of Figure 1B). As we known, a nonbridging oxygen of the phosphate backbone is substituted

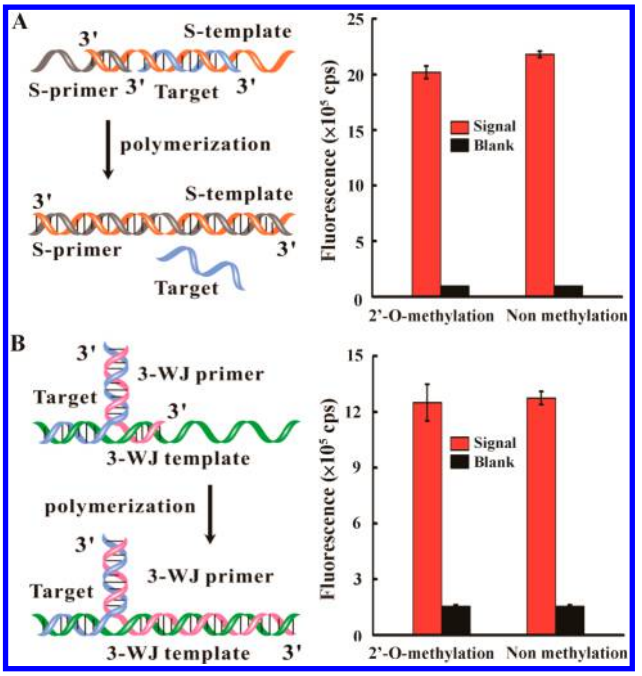

Figure 4. Schematic representation (left) and corresponding fluorescence response (right) of SDA for the unbiased recognition of 3′-terminal 2′-O-methylated small RNA by base-stacking hybridization (A) and 3-WJ structure (B).

by a sulfur atom in phosphorothioate modification, rendering the internucleotide linkage resistant to enzymatic degradation. Since the cleavage product by nicking enzyme is the same as that of enzymatic degradation (with 3′-OH and 5′-phosphate), we surmise that phosphorothioate modification also help inhibit attack by nicking enzyme. Therefore, a trifunctional stem-loop template containing a hemiphosphorothioate nicking site is tactfully designed (Figure 1B and Figure S4). It contains three characteristic parts with different functions. With I portion, this template recognizes target RNA and then forms stable 3-WJ structure with 3-WJ primer. Once the polymerization reaction is initiated, a duplex template containing two full nicking sites is formed. One (III) of them is of phosphorothioate-modified which cannot be cut by nicking enzyme. Oppositely, another one (II) is nicked (first nicking position), resulting in the generation of new 3′-OH. This 3′-OH then induces next polymerization reaction with the displacement of the single-stranded product (ss-product). Thus, lots of ss-products are accumulated owing to the repeat process of polymerization and nicking. As signal reporter, MB containing the same nicking site is designed to be complementary with the ss-product. After stable hybridization with ss-product, the MB is turned into duplex structure with double-stranded nicking site (Figure S5). As the MB is nicked (second nicking position), it is dissociated from the duplex structure accompanied by the release of ss-product, resulting in the restoration of fluorescence signal. Subsequently, the released ss-product can then hybridize with another MB and induce the second cycle of cleavage. Eventually, one target molecule can result in the generation of many ss-products, and each ss-product can also undergo plenty of cleavage cycles of MB, affording a high quadratically amplified signal. Compared to the method[36] previously reported by our group which needs complex design of additional hairpin probe to connect MB and ss-product, this strategy is much simpler.

DOI: 10.1021/acs.analchem.5b01683
Anal. Chem. 2015, 87, 8758−8764

Exactly as we speculate, phosphorothioate modification in nicking site of the 3T-PS template (Figure S6) was proved to really inhibit the nicking reaction (Figure 5A). And the

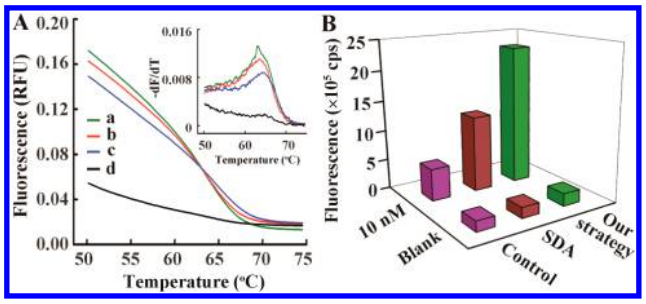

Figure 5. Feasibility of the proposed PS−PBN strategy. (A) The analysis of nicking reaction of different templates by melting curve. The letters a−d represent the samples of 3T-PS template (Table S1) without nicking enzyme, 3T-PS template with nicking enzyme, 3T template without nicking enzyme, and 3T template with nicking enzyme, respectively. Inset is the corresponding melting peaks. (B) The fluorescence response of 3T template system (control), 3-WJ template system (SDA), and 3T-PS template system (Our strategy, PS−PBN).

fluorescence intensity triggered by this trifunctional template is much higher than those of the SDA template and the nonphosphorothioate trifunctional template (Figures 5B, S7, and S8), demonstrating the high amplified signal by our strategy. To obtain the highest sensing performance, the effects of the several important conditions were investigated. Since polymerase catalyzes polymerization reaction, its concentration was first studied. As we expected, a higher polymerase concentration leads to a higher fluorescence signal (Figure 6A). However, a relatively strong fluorescence intensity of background was also observed as its concentration increased. Due to the highest F/F_0, 0.5 units of KF^- was selected as the optimized concentration. As nicking enzyme carry out the cleavage of both template duplex and MB, its concentration is significant in the sensing system. As presented in Figure 6B, a high concentration of Nt.BbvCI results in the strong fluorescence response. Unfortunately, the fluorescence intensity without target is also enhanced with the increase of Nt.BbvCI concentration. Thus, we used 2.5 units of Nt.BbvCI for the following experiments. As we described above, the ss-product (3T product) can hybridize with MB to trigger the nicking of MB. However, it is also complementary to the excess 3T-PS template, which may lost the assay sensitivity. We hypothesize that using 3T product to form stable heteroduplex with 3T-PS template can prevent the ss-product from hybridizing to 3T-PS template, resulting in the increase of sensitivity. This hypothesis is confirmed as depicted in Figure 6C. The ratio value of 0.25:1 is chose due to the highest F/F_0 value.

Under optimized conditions, a series of samples containing various target concentrations were tested to evaluate the sensing sensitivity. It can be seen in Figure 7A, the fluorescence intensity rises gradually with the corresponding increase of target concentrations. The value of fluorescence intensity is linearly associated with the logarithm (lg) of target concentration ranging from 4 pM to 500 pM, with a correlation equation of $F = 7.24 + \lg C$ (nM) ($R^2 = 0.990$), whereas C represent the target concentration. The detection limit of 600 fM was achieved based on 3σ method within 30 min. It is notable that this time is much shorter than those of many

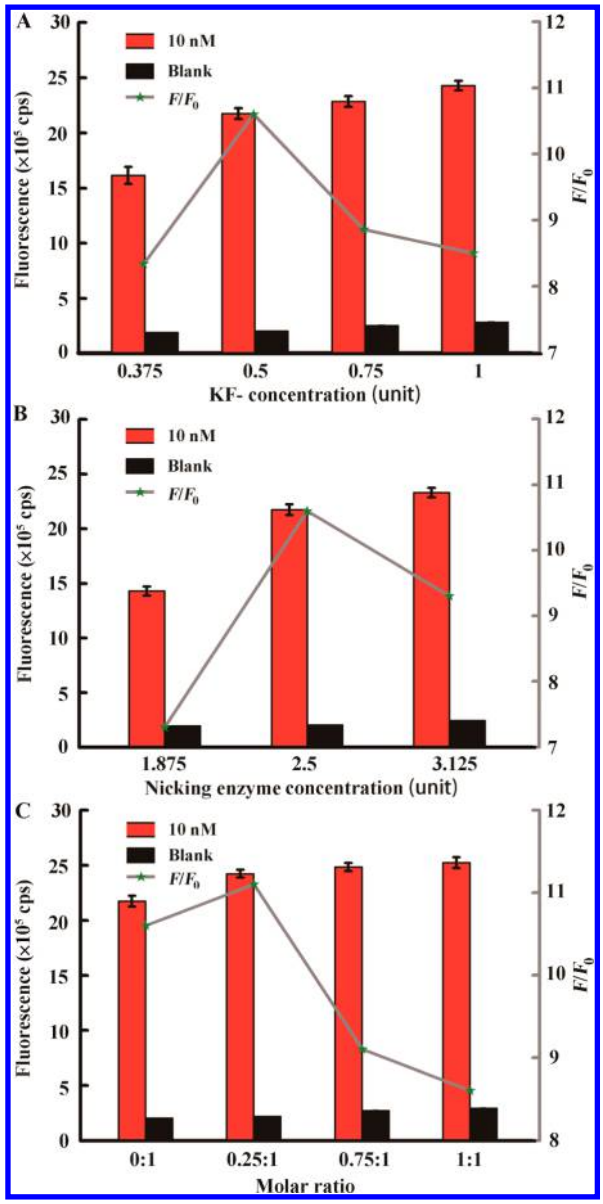

Figure 6. Optimization of the experimental conditions. The effect of KF^- concentration (A), Nt.BbvCI concentration (B), and molar ratio of 3T product to 3T-PS template (C) on the fluorescence response of the sensing system, respectively.

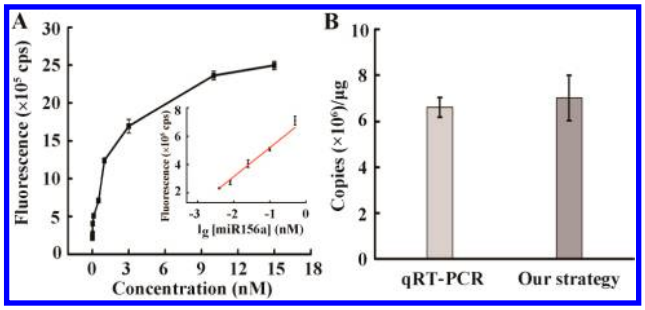

Figure 7. Performance of the proposed PS−PBN strategy. (A) Fluorescence response to different target concentrations by PS−PBN. The inset displays the linear correlation between the fluorescence intensity and the logarithm of the target concentration in the range of 4−500 pM. (B) Performance in the analysis of small RNAs sample extracted from *Arabidopsis thaliana*.

DOI: 10.1021/acs.analchem.5b01683
Anal. Chem. 2015, 87, 8758−8764

reported methods,[20,22,37−39] and lengthening the assay time is able to significantly increase the sensitivity.[16] For the further validation of the method, RNA samples extracted from *Arabidopsis thaliana* was analyzed by the proposed method (Figure S9). And as shown in Figure 7B, the obtained result of small RNA sample was in agreement with that by reverse transcription-PCR based method (Figures S10 and S11).[40] It is worthy to point out that this PCR-based method is not affected by 3′-terminal 2′-O-methylation via using small RNA as template rather than primer (Figure S10). However, the additional reverse transcription step suffers from incomplete reverse of RNA into complementary DNA as well as lengthy assay time (about 1 h), and even may increase RNase contamination. Furthemore, it requires precision temperature cycling process in a costly thermocycler compared to our developed isothermal strategy.

CONCLUSIONS

In summary, we systematically investigated the impact of 3′-terminal 2′-O-methylated small RNAs on target-primed polymerization reaction. We observed that this modification remarkably suppresses the polymerization reactions catalyzed by three representative DNA polymerases, causing biased analysis results. The potential mechanism of such inhibition have been discussed and clarified. Subsequently, two novel solutions each using base-stacking hybridization and 3-WJ structure have been proposed to circumvent this suppression impact and achieve unbiased recognition. Furthermore, great effort has been devoted to the development of a creative amplified strategy PS−PBN by designing a trifunctional stem-loop phosphorothioate template. Small RNA samples of *Arabidopsis thaliana* were successfully detected, holding powerful implications in practical application. Collectively, this study presents mechanistic insight into the suppression impact of enzymatic polymerization by 3′-terminal 2′-O-methylated small RNAs, and provides unbiased solutions for the amplified quantification of small RNAs. Our ongoing work will expand the proposed strategy for the analysis of other important small RNAs and investigate their biological function.

ASSOCIATED CONTENT

Supporting Information

The Supporting Information is available free of charge on the ACS Publications website at DOI: 10.1021/acs.analchem.5b01683.

Experimental procedures and analytical data (PDF)

AUTHOR INFORMATION

Corresponding Author

*E-mail: yxzhao@mail.xjtu.edu.cn. Fax: 86-29-82663454.

Notes

The authors declare no competing financial interest.

ACKNOWLEDGMENTS

This research was financially supported by the National Natural Science Foundation of China (21475102 and 21005059) and the Fundamental Research Funds for the Central Universities (xjj2014130).

REFERENCES

(1) Ghildiyal, M.; Zamore, P. D. *Nat. Rev. Genet.* **2009**, *10*, 94−108.
(2) Siomi, M. C.; Sato, K.; Pezic, D.; Aravin, A. A. *Nat. Rev. Mol. Cell Biol.* **2011**, *12*, 246−258.
(3) Kim, V. N.; Han, J.; Siomi, M. C. *Nat. Rev. Mol. Cell Biol.* **2009**, *10*, 126−139.
(4) Small, E. M.; Olson, E. N. *Nature* **2011**, *469*, 336−342.
(5) Zhao, C.; Sun, G.; Li, S.; Lang, M. F.; Yang, S.; Li, W.; Shi, Y. *Proc. Natl. Acad. Sci. U. S. A.* **2010**, *107*, 1876−1881.
(6) Castel, S. E.; Martienssen, R. A. *Nat. Rev. Genet.* **2013**, *14*, 100−112.
(7) Dunoyer, P.; Schott, G.; Himber, C.; Meyer, D.; Takeda, A.; Carrington, J. C.; Voinnet, O. *Science* **2010**, *328*, 912−916.
(8) Sarkies, P.; Miska, E. A. *Nat. Rev. Mol. Cell Biol.* **2014**, *15*, 525−535.
(9) Esteller, M. *Nat. Rev. Genet.* **2011**, *12*, 861−874.
(10) Yu, B.; Yang, Z.; Li, J.; Minakhina, S.; Yang, M.; Padgett, R. W.; Steward, R.; Chen, X. *Science* **2005**, *307*, 932−935.
(11) Li, J.; Yang, Z.; Yu, B.; Liu, J.; Chen, X. *Curr. Biol.* **2005**, *15*, 1501−1507.
(12) Tian, Y.; Simanshu, D. K.; Ma, J. B.; Patel, D. J. *Proc. Natl. Acad. Sci. U. S. A.* **2011**, *108*, 903−910.
(13) Ji, L.; Chen, X. *Cell Res.* **2012**, *22*, 624−636.
(14) Tian, L. L.; Cronin, T. M.; Weizmann, Y. *Chem. Sci.* **2014**, *5*, 4153.
(15) Shlyahovsky, B.; Li, D.; Weizmann, Y.; Nowarski, R.; Kotler, M.; Willner, I. *J. Am. Chem. Soc.* **2007**, *129*, 3814−3815.
(16) Hsieh, K.; Patterson, A. S.; Ferguson, B. S.; Plaxco, K. W.; Soh, H. T. *Angew. Chem.* **2012**, *124*, 4980−4984.
(17) Lei, C. Y.; Huang, Y.; Nie, Z.; Hu, J.; Li, L. J.; Lu, G. Y.; Han, Y. T.; Yao, S. Z. *Angew. Chem.* **2014**, *126*, 8498−8502.
(18) Jou, A. F.; Lu, C. H.; Ou, Y. C.; Wang, S. S.; Hsu, S. L.; Willner, I.; Ho, J. A. *Chem. Sci.* **2015**, *6*, 659−665.
(19) Jia, H.; Li, Z.; Liu, C.; Cheng, Y. *Angew. Chem., Int. Ed.* **2010**, *49*, 5498−5501.
(20) Yin, B. C.; Liu, Y. Q.; Ye, B. C. *Anal. Chem.* **2013**, *85*, 11487−11493.
(21) Duan, R.; Zuo, X.; Wang, S.; Quan, X.; Chen, D.; Chen, Z.; Jiang, L.; Fan, C.; Xia, F. *J. Am. Chem. Soc.* **2013**, *135*, 4604−4607.
(22) Zhou, D. M.; Du, W. F.; Xi, Q.; Ge, J.; Jiang, J. H. *Anal. Chem.* **2014**, *86*, 6763−6767.
(23) Degliangeli, F.; Kshirsagar, P.; Brunetti, V.; Pompa, P. P.; Fiammengo, R. *J. Am. Chem. Soc.* **2014**, *136*, 2264−2267.
(24) Shi, C.; Liu, Q.; Ma, C.; Zhong, W. *Anal. Chem.* **2014**, *86*, 336−339.
(25) Dong, H.; Lei, J.; Ding, L.; Wen, Y.; Ju, H.; Zhang, X. *Chem. Rev.* **2013**, *113*, 6207−6233.
(26) Munafó, D. B.; Robb, G. B. *RNA* **2010**, *16*, 2537−2552.
(27) Kaul, C.; Müller, M.; Wagner, M.; Schneider, S.; Carell, T. *Nat. Chem.* **2011**, *3*, 794−800.
(28) Funai, T.; Nakamura, J.; Miyazaki, Y.; Kiriu, R.; Nakagawa, O.; Wada, S. I.; Ono, A.; Urata, H. *Angew. Chem., Int. Ed.* **2014**, *53*, 6624−6627.
(29) Crespo-Hernández, C. E.; Cohen, B.; Kohler, B. *Nature* **2005**, *436*, 1141−1144.
(30) Zhao, Y.; Qi, L.; Chen, F.; Zhao, Y.; Fan, C. *Biosens. Bioelectron.* **2013**, *41*, 764−770.
(31) Zhang, D. Y.; Winfree, E. *J. Am. Chem. Soc.* **2009**, *131*, 17303−17314.
(32) Zhang, D. Y.; Chen, S. X.; Yin, P. *Nat. Chem.* **2012**, *4*, 208−214.
(33) Li, B.; Jiang, Y.; Chen, X.; Ellington, A. D. *J. Am. Chem. Soc.* **2012**, *134*, 13918−13921.
(34) Shu, D.; Shu, Y.; Haque, F.; Abdelmawla, S.; Guo, P. *Nat. Nanotechnol.* **2011**, *6*, 658−667.
(35) Oleksi, A.; Blanco, A. G.; Boer, R.; Usón, I.; Aymamí, J.; Rodger, A.; Hannon, M. J.; Coll, M. *Angew. Chem.* **2006**, *118*, 1249−1253.
(36) Zhao, Y.; Chen, F.; Zhang, Q.; Zhao, Y.; Zuo, X.; Fan, C. *NPG Asia Mater.* **2014**, *6*, e131−e131.
(37) Zhang, Y.; Zhang, C. Y. *Anal. Chem.* **2012**, *84*, 224−231.
(38) Liu, H.; Li, L.; Duan, L.; Wang, X.; Xie, Y.; Tong, L.; Wang, Q.; Tang, B. *Anal. Chem.* **2013**, *85*, 7941−7947.

DOI: 10.1021/acs.analchem.5b01683
Anal. Chem. 2015, 87, 8758−8764

(39) Ren, Y.; Deng, H. M.; Shen, W.; Gao, Z. Q. *Anal. Chem.* **2013**, *85*, 4784−4789.
(40) Chen, C.; Ridzon, D. A.; Broomer, A. J.; Zhou, Z.; Lee, D. H.; Nguyen, J. T.; Barbisin, M.; Xu, N. L.; Mahuvakar, V. R.; Andersen, M. R. *Nucleic Acids Res.* **2005**, *33*, e179−e179.

DOI: 10.1021/acs.analchem.5b01683
Anal. Chem. 2015, 87, 8758−8764